Autophagy Inhibition Enables Nrf2 to Exaggerate the Progression of Diabetic Cardiomyopathy in Mice

Huimei Zang,[1] Weiwei Wu,[1] Lei Qi,[1] Wenbin Tan,[1] Prakash Nagarkatti,[2] Mitzi Nagarkatti,[2] Xuejun Wang,[3] and Taixing Cui[1]

Diabetes 2020;69:2720–2734 | https://doi.org/10.2337/db19-1176

Nuclear factor-erythroid factor 2–related factor 2 (Nrf2) may either ameliorate or worsen diabetic cardiomyopathy. However, the underlying mechanisms are poorly understood. Herein we report a novel mechanism of Nrf2-mediated myocardial damage in type 1 diabetes (T1D). Global Nrf2 knockout (Nrf2KO) hardly affected the onset of cardiac dysfunction induced by T1D but slowed down its progression in mice independent of sex. In addition, Nrf2KO inhibited cardiac pathological remodeling, apoptosis, and oxidative stress associated with both onset and advancement of cardiac dysfunction in T1D. Such Nrf2-mediated progression of diabetic cardiomyopathy was confirmed by a cardiomyocyte-restricted (CR) Nrf2 transgenic approach in mice. Moreover, cardiac autophagy inhibition via CR knockout of autophagy-related 5 gene (CR-Atg5KO) led to early onset and accelerated development of cardiomyopathy in T1D, and CR-Atg5KO–induced adverse phenotypes were rescued by additional Nrf2KO. Mechanistically, chronic T1D leads to glucolipotoxicity inhibiting autolysosome efflux, which in turn intensifies Nrf2-driven transcription to fuel lipid peroxidation while inactivating Nrf2-mediated antioxidant defense and impairing Nrf2-coordinated iron metabolism, thereby leading to ferroptosis in cardiomyocytes. These results demonstrate that diabetes over time causes autophagy deficiency, which turns off Nrf2-mediated defense while switching on an Nrf2-operated pathological program toward ferroptosis in cardiomyocytes, thereby worsening the progression of diabetic cardiomyopathy.

Diabetic cardiomyopathy is a clinical myocardial condition distinguished by cardiac hypertrophy and fibrosis, as well as an early onset of ventricular diastolic dysfunction and late onset of ventricular systolic dysfunction, in the absence of changes in blood pressure and coronary disease (1). The pathogenesis of diabetic cardiomyopathy is multifactorial and complicated, but oxidative stress, a result of an imbalance between the production of reactive oxygen species and the antioxidant capacity, has been widely accepted as a common mechanism leading to diabetic cardiomyopathy (2,3). Extensive studies have revealed that an effective therapy for diabetic cardiomyopathy requires either specific targeting of the source of oxidative stress or endogenous antioxidant defense system, rather than nonselective scavenging of reactive oxygen species that may compromise physiological redox signaling (2).

Nuclear factor-erythroid factor 2–related factor 2 (Nrf2), a transcription factor, controls the basal and inducible expression of >1,000 genes that can be grouped into several categories including antioxidant genes, phase II detoxifying enzymes, transcriptional factors, transporters, scavenger receptors, proteasomal and autophagic degradation, and metabolism (4). Thus, the functions of Nrf2 spread rather broadly from antioxidant defense to protein quality control and metabolism regulation. Nevertheless, Nrf2 has historically been considered as a master regulator of antioxidant defense and has evolved into a promising drug target for the treatment of human diseases associated with oxidative stress, such as diabetic cardiomyopathy (5). However, existing literatures regarding the role of Nrf2 in diabetes per se and diabetes complications have been very controversial. For example, genetic activation of Nrf2 by globally hypomorphic knockdown of Kelch-like ECH-associated protein 1 (Keap1), an endogenous inhibitor of

[1]Department of Cell Biology and Anatomy, School of Medicine, University of South Carolina, Columbia, SC
[2]Department of Pathology, Microbiology and Immunology, School of Medicine, University of South Carolina, Columbia, SC
[3]Division of Basic Biomedical Sciences, University of South Dakota Sanford School of Medicine, Vermillion, SD
Corresponding author: Taixing Cui, taixing.cui@uscmed.sc.edu

Received 26 November 2019 and accepted 10 September 2020

This article contains supplementary material online at https://doi.org/10.2337/figshare.12937733.

Nrf2, suppresses the onset of diabetes in *db/db* mice (6) while paradoxically worsening the insulin resistance and glucose intolerance in *ob/ob* mice (7). In addition, knockout (KO) of Nrf2 globally or specifically in adipocytes reduces white adipose tissue mass but resulting in severe metabolic syndrome with aggravated insulin resistance, hyperglycemia, and hypertriglyceridemia in *ob/ob* mice (8). Moreover, either a protective or detrimental role of Nrf2 in type 1 diabetes (T1D)-induced nephropathy is documented by two independent laboratories using the same global Nrf2 knockout (Nrf2KO) approach in mice (9,10). Similarly, a cardiac protective role of Nrf2 is noticed in both type 1 and type 2 diabetic mice (11,12), whereas a detrimental axis of cardiac Nrf2-CD36-lipotoxicity is also observed in type 1 diabetic fibroblast growth factor 21 (Fgf21) KO mice (13). The precise reasons underlying these discrepancies remain unknown.

Autophagy is an evolutionarily conserved pathway that targets cytoplasmic contents to the lysosome for degradation (14). Based on the means by which the target is delivered into lysosomes for final degradation, autophagy has been classified into three types: *1*) macroautophagy, *2*) microautophagy, and *3*) chaperone-mediated autophagy. The macroautophagy (hereafter referred to as autophagy) is the best characterized. Systemic autophagy inhibition induces premature aging and shortens the life span whereas cardiac-specific autophagy inhibition causes age-related cardiomyopathy and death in nondiabetic settings (15). Both type 1 and 2 diabetic settings in mice result in myocardial autophagy inhibition (16–18). The cardiac autophagy inhibition in most type 2 diabetes models seems to be maladaptive; however, the cardiac autophagy inhibition in type 1 diabetes models appears to be either adaptive or maladaptive depending on the nature of diabetes settings (16,17). The exact role of autophagy in diabetic cardiomyopathy particularly associated with T1D remains to be addressed.

We have uncovered that Nrf2 mediates dichotomous effects on the heart depending on the functional status of myocardial autophagy in a nondiabetic setting of pressure overload (19). Activation of Nrf2 is cardioprotective when myocardial autophagy function is intact, but it becomes detrimental when myocardial autophagy function is insufficient (19). Therefore, we questioned whether such an Nrf2-mediated dichotomy could be extrapolated into the pathogenesis of diabetic cardiomyopathy in which cardiac autophagy gradually becomes compromised in chronic diabetes settings (16,17). In the current study, we demonstrate that cardiac autophagy inhibition activates Nrf2-mediated myocardial damage via a mechanism that enables Nrf2-mediated ferroptosis in cardiomyocytes, thereby exaggerating the progression of cardiomyopathy associated with T1D.

RESEARCH DESIGN AND METHODS

Animals

The breeding pairs of global Nrf2 heterozygote KO and floxed autophagy-related 5 ($Atg5^{fl/fl}$) mice on a C57BL/6J genetic background were purchased from RIKEN BioResource Research Center, Tsukuba, Ibraraki, Japan. The breeding pairs of a transgenic mouse strain harboring a tamoxifen-inducible Cre-fusion protein (MerCreMer) under the control of cardiomyocyte-specific α-myosin heavy-chain promoter (Myh6 or αMHC) on a C57BL/6J genetic background were purchased from The Jackson Laboratory. Littermates of wild-type (WT) and global Nrf2KO, MerCreMer control ($MerCreMer^{+}$), $MerCreMer^{+}$::Nrf2KO, $MerCreMer^{+}$::($Atg5^{fl/fl}$), and $MerCreMer^{+}$::$Atg5^{fl/fl}$::Nrf2KO mice on a C57BL/6J genetic background were generated as we previously described (19). The induction of Cre-loxP recombination in mice was carried out via an optimized tamoxifen treatment regimen, i.e., intraperitoneal (i.p.) injection of tamoxifen at 20 mg/kg body weight (BW) daily (20 mg/kg/day) for 21 days, which induces MerCreMer-mediated ablation of Atg5 gene in cardiomyocytes of adult mice without detectable toxic effects at the baseline (19). Littermates of nontransgenic WT control (NG) and cardiomyocyte-restricted (CR) Nrf2 transgenic (TG) mice on a FVB/N genetic background were generated as we previously described (20). All mice at age of 8 weeks, if not specified, were used for experiments. All animals were housed at the AAALAC-accredited animal facility of University of South Carolina School of Medicine. All animals were treated in compliance with the National Institutes of Health Guideline for the Care and Use of Laboratory Animals. The use of animals and all animal procedures were approved by the Institutional Animal Care and Use Committee at University of South Carolina.

T1D Model

T1D in mice was induced by five consecutive injections (i.p.) of 50 mg/kg/day streptozotocin (STZ), the low-dose protocol that is recommended by the Animal Models of Diabetic Complication Consortium (AMDCC) to minimize the off-target effect of STZ (21). After STZ injection, BW and blood glucose levels were monitored daily within the 1st week and weekly from the 2nd week to the end of the 1st month and then monthly from the 2nd month to the experimental end points. Diabetes was diagnosed by three consecutive measures of nonfasting blood glucose level >16.4 mmol/L, and the 7th day after STZ injection was considered as onset (0 day) of diabetes. i.p. glucose tolerance test was performed by measurement of blood glucose levels at 0, 15, 30, 120, and 180 min after injection (i.p.) of 20% D-glucose in saline at a dose of 2 g/kg in 14-h-fasted nonanesthetized mice. Blood glucose levels were measured by Accu-Check Aviva glucometers (Roche). Blood triglyceride and cholesterol levels were measured with a cholesterol assay kit (cat. no. ab65390; Abcam) and a triglyceride colorimetric assay kit (cat. no. 10010303; Cayman Chemical).

Echocardiography

Echocardiography was performed on anesthetized mice using the VisualSonics Vevo 2100 system (VisualSonics, Inc.) equipped with a 30-MHz frequency linear transducer as we previously described (19,20).

Cardiac Autophagic Flux Assessment In Vivo

Autophagic flux was measured by the difference of microtubule-associated proteins 1A/1B light chain 3 (LC3)-II protein levels in the absence or presence of bafilomycin A1 (BafA1), an inhibitor of autophagosome fusion with lysosomes (19,22). Mice were injected (i.p.) with vehicle DMSO control or BafA1 at a dose of 6 μmol/kg BW in DMSO for 30 min and then euthanized for the assessment of myocardial LC3-II levels.

Pathology and Histological and Biochemical Analyses

Gross pathologies, cardiac hypertrophy, fibrosis, apoptosis, oxidative stress, iron deposition, and myocardial protein and mRNA expression were assessed as we previously described (19,20). Iron deposition was measured by Prussian blue staining at an iron stain kit (cat. no. ab150674; Abcam). For histological and immunochemical analyses, hearts were cannulated via the left ventricle (LV) apex, cleared by perfusion with saline (0.9% NaCl) at 90 mmHg, arrested in diastole with 10% KCl (w/v in double-distilled H_2O), fixed by perfusion with 4% paraformaldehyde, and embedded in paraffin. Paraffin sections were prepared (5 μm) and stored at room temperature until staining. Cardiomyocyte cross-sectional area and cardiac fibrosis, apoptosis, oxidative stress, and iron deposition in LVs were quantified. For Western blot and quantitative real-time PCR (qPCR) analyses, hearts were cannulated via the LV apex and cleared by perfusion with saline (0.9% NaCl) at 90 mmHg, and then the LVs were dissected, frozen, and stored in liquid nitrogen. Total proteins or RNAs of LVs were extracted for the assessments. The antibodies that were used for immunochemical staining and Western blot analysis are summarized in Supplementary Table 1. The primers for qPCR are summarized in Supplementary Table 2.

Cell Culture, Autophagosome Flux and Autolysosome Efflux Assessments, and Cytotoxicity Assay In Vitro

Rat H9C2 cells, a myoblast cell line derived from embryonic rat hearts that maintains some feature of cardiac myocytes (cat. no. CRL-1466; ATCC), were cultured in DMEM (1 g/L or 5.5 mmol/L glucose) supplemented with 10% FBS under an atmosphere of 5% CO_2 and 95% O_2 at 37°C. Assessments of the impact of glucotoxicity, lipotoxicity, and glucolipotoxicity on autophagosome flux and autolysosome efflux; the effect of Atg5 knockdown on glucotoxicity, lipotoxicity, and glucolipotoxicity; and the effect of Nrf2 knockdown on ferroptosis in H9C2 cardiomyocyte-like cells were carried out as we previously reported (19,22). Briefly, H9C2 cells at 95% confluent state were subject to the following experiments: *1*) Autophagosome flux and autolysosome efflux. H9C2 cells were transfected with mCherry-Gfp-Lc3 plasmids (123230; Addgene, Cambridge, MA) with use of Lipofectamine 3000 reagent (L30000015; Thermo Fisher Scientific) for 24 h and then cultured for an additional 24 h in serum-free DMEM with normal glucose (5.5 mmol/L), high glucose (35.5 mmol/L) to mimic glucotoxicity, lipid palmitic acids (PAs) (500 μmol/L) overloading to mimic lipotoxicity, or high glucose with PA overloading to mimic glucolipotoxicity until the assessment. Mannitol (30 mmol/L + 5.5 mmol/L glucose) was used to normalize the impact of osmotic effect of high-glucose setting in the control groups. The cellular effects of BSA per se was considered by addition of the same amount of BSA in the control groups. BafA1 (10 nmol/L) was also added for 24 h to block autophagosomes fusion with minimal affecting of lysosomal degradation of autolysosomes. *2*) Atg5 and Nrf2 knockdown. H9C2 cells were transfected with small-interfering control (5′-CGUACGCG GAAUACUUCGATT-3′, Integrated DNA Technologies), siAtg5 (5′-GACGCUGGUAACUGACAAATT-3′, Integrated DNA Technologies), and siNrf2 (no. 1, 5′-GCAUGUU ACGUGAUGAGGA-3′ [cat. no. s136129; Thermo Fisher Scientific]; no. 2, 5′-CAAGAAGCCAGAUACAAA-3′, IDT; and no. 3, 5′-GCUGAACUCCUUAGACUCA-3′ [cat. no. s136127; Thermo Fisher Scientific]) RNAs. Cells were treated with erastin or deferoxamine as indicated in serum-free DMEM for 24 h. Cytotoxicity was assessed by measuring LDH release and propidium iodide (PI) (cat. no. AS-83215; AnaSpec, Inc.) staining.

Statistics

Data are shown as mean ± SD. Differences between two groups were evaluated for statistical significance using the Student *t* test. When differences among more than three groups were evaluated, results were compared by one-way ANOVA with Bonferroni test for multiple comparisons. Survival rates between experimental groups were analyzed using Kaplan-Meier test. Differences were considered significant at $P < 0.05$.

Data and Resource Availability

All data generated and analyzed during this study are included in the published article and supplementary material.

RESULTS

A Mediator Role of Cardiac Nrf2 in the Progression of Cardiomyopathy Associated With T1D

To characterize the role of Nrf2 in diabetic cardiomyopathy, we carried out a time course study with the end points of 0, 1, 3, 6, and 9 months after onset of STZ-induced diabetes using adult male and female WT and Nrf2KO mice. We found that *1*) diabetes-associated death was increased in Nrf2KO mice compared with WT mice, whereas the increase in fasting glucose level and diabetes-associated decrease in BW were improved by Nrf2KO in both male (Fig. 1*A* and Supplementary Fig. 1) and female (Supplementary Fig. 2) mice, and *2*) Nrf2KO did not affect the onset of cardiac dysfunction at 6 months but slowed down the progression of cardiac dysfunction at 9 months in both male (Fig. 1*C*) and female (Supplementary Fig. 9) mice. In addition, myocardial hypertrophy, cell death, fibrosis, and oxidative stress at middle (6 months) and later (9 months) stages, but not at early stages (0–3 months), of diabetes were attenuated by Nrf2KO in both male (Fig. 2

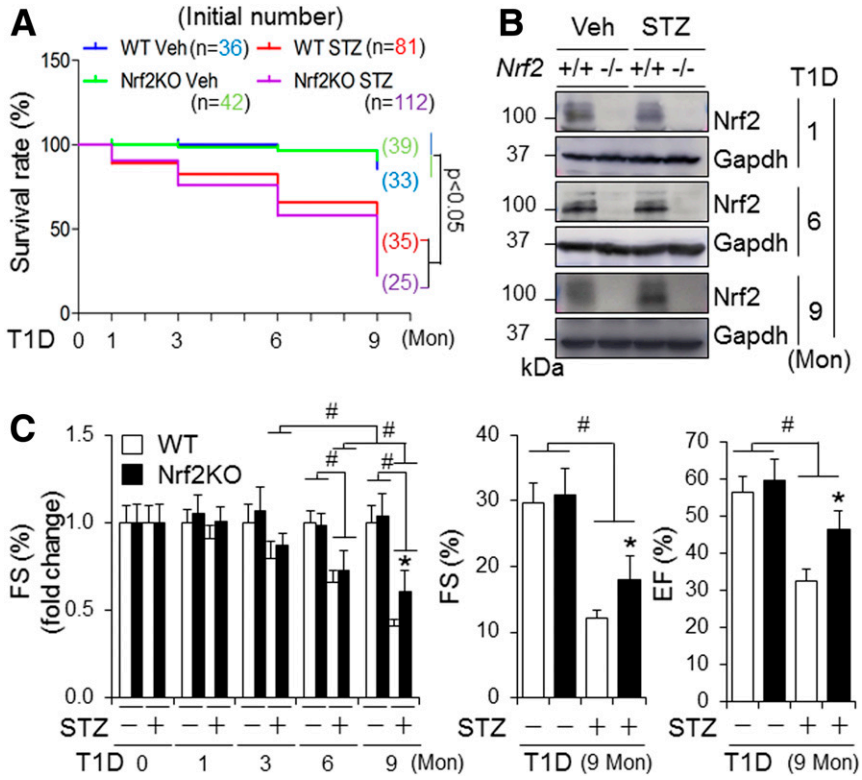

Figure 1—The impact of global KO of Nrf2 on survival rate and cardiac function in mice with STZ-induced diabetes. T1D in littermates of adult male WT and Nrf2KO mice on a C57BL/6J genetic background was induced by i.p. injection of STZ for 9 months (Mon) as described in RESEARCH DESIGN AND METHODS. *A*: Kaplan-Meier analysis of survival rate. Veh, vehicle treated. *B*: Representative immunoblots of myocardial Nrf2. WT, $Nrf2^{+/+}$; Nrf2KO, $Nrf2^{-/-}$. *C*: Cardiac function. Left panel shows a time course study of FS (%) in fold changes. Right panel shows arbitrary FS (%) and ejection fraction (EF) (%) at 9 months. #$P < 0.05$ between indicated groups; *$P < 0.05$ vs. WT STZ groups at 9 months. Animal numbers for each group (*A–C*) are indicated in Supplementary Fig. 1*A*.

and Supplementary Figs. 3–8) and female (Supplementary Figs. 10–15) mice. Of note, there was physiological cardiac growth in these mice from age 2 months to age 11 months and BW of Nrf2KO mice was slightly lower than that of their WT littermates at the basal condition (Supplementary Figs. 1*B*, 2*B*, and 16). To avoid potential effects of these interferences on experimental results over a time period of 9 months, we compared the fold changes of fractional shorting (FS) (%), BW, and heart weight–to–tibia length ratios in this time course study. Taken together, these results reveal that Nrf2 provides a general protection against T1D onset and its associated death; however, it does not prevent or delay the development of cardiomyopathy associated with T1D; instead, it may facilitate its progression independent of sex differences. At the molecular level, Nrf2 may activate a mechanism that enhances oxidative stress in the diabetic heart, thereby promoting the progression of diabetic cardiomyopathy.

Cardiac Autophagy Inhibition Is Maladaptive in T1D

To date, the dynamics of myocardial autophagy inhibition in T1D have not been well characterized, while the critical cause and precise role of myocardial autophagy inhibition in cardiomyopathy associated with T1D remain unclear (16,17). Therefore, we performed a time course study of myocardial autophagic flux, a more accurate parameter reflecting autophagy functional status, during a chronic setting of STZ-induced T1D in mice, and then determined the impact of hyperglycemia and/or lipid overloading on autophagic flux in vitro, which mimics glucotoxicity, lipotoxicity, and glucolipotoxicity, respectively (23). Moreover, we examined the impact of myocardial autophagy inhibition induced via CR knockout of autophagy-related 5 gene (CR-Atg5KO) on T1D-induced cardiomyopathy in adult mice.

We found that cardiac autophagic flux is intact at 3 months but is dramatically suppressed at 6 months after onset of diabetes (Fig. 3*A*) associated with intensified increases in triglycerides and cholesterol (Supplementary Table 3) as observed in C57BL/6J mice (23), indicating a contributory role of hyperlipidemia in inhibiting myocardial autophagy in T1D. On the other hand, we established an experimental system for quantifying autophagosome flux and autolysosome efflux in H9C2 cardiomyocyte-like cells expressing the mCherry-Gfp-Lc3 reporter (Fig. 3*B*) as we previously described (22). The green fluorescent signal of GFP is quenched by the low pH inside the lysosome, whereas red fluorescent signal of mCherry exhibits more stable fluorescence in the acidic compartment of cells. As a result,

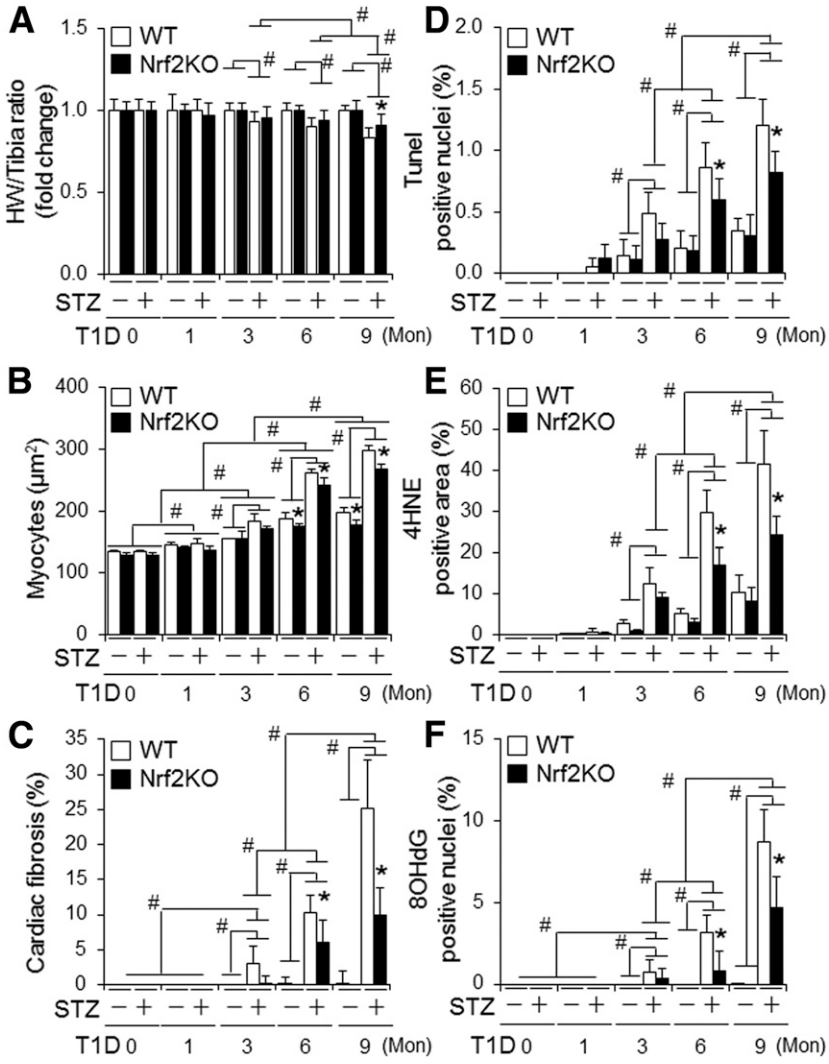

Figure 2—The impact of global KO of Nrf2 on cardiac remodeling, apoptosis, and oxidative stress in mice with STZ-induced diabetes. T1D in littermates of adult male WT and Nrf2KO mice on a C57BL/6J genetic background was induced by i.p. injection of STZ for 9 months (Mon) as described in RESEARCH DESIGN AND METHODS. *A*: Heart weight (HW)–to–tibia length ratio in fold changes. The values of vehicle-treated groups are set as onefold. #$P < 0.05$ between indicated groups; *$P < 0.05$ vs. WT STZ group at 9 months. Animal numbers for each group are indicated in Supplementary Fig. 1*A*. *B*: Cardiomyocyte sizes. *C*: Cardiac fibrosis (%). *D*: Cardiac apoptosis. *E* and *F*: Cardiac oxidative stress assessed by quantifying the percentage of 4HNE-positive areas and 8OHdG-positive stained nuclei, respectively. LV tissue sections of the WT and Nrf2KO mice were used for the assessments from *B* to *F*. *B–F*: Animal numbers for each group are 3–5. *B–F*: #$P < 0.05$ between indicated groups. *$P < 0.05$ vs. WT STZ groups at the same end points.

autolysosomes are marked by red fluorescence alone, whereas autophagosomes are labeled with yellow fluorescence (red and green fluorescence). In a setting of 24 h culture in serum-free normal-glucose DMEM, the constitutive (basal) autophagy in H9C2 cells was characterized by a preponderance of autolysosomes (punctate dots red only) and a few autophagosomes (yellow punctate dots) (Fig. 3*B*), indicating a status in which most of the synthesized autophagosomes are constantly fused with lysosomes to form autolysosomes for autolysosomal degradation. Thus, we controlled the autophagy status with an optimized dose of a lysosome inhibitor, BafA1 (10 nmol/L) to differentiate the amount of autophagosomes to be fused with lysosomes, i.e., autophagosome flux (BafA1-induced accumulation of autophagosomes), as well as the amount of autophagosomes fused with lysosomes to be degraded, i.e., autolysosomal degradation or autolysosome efflux (BafA1-induced down-regulation of autolysosomes) (22). Accordingly, we found that palmitate overloading, but not high glucose (typical images not shown), suppresses autophagy characterized by impaired autolysosomal efflux in H9C2 cells, and the lipid overload-induced autophagy inhibition is worsened in a high-glucose milieu (Fig. 3*B*). In addition, it is palmitate overload but not high glucose that inhibits autophagic flux (LC3-II accumulation induced by chloroquine, another lysosome inhibitor), and such lipid overload–induced inhibition of autophagic flux is enhanced by a high-glucose milieu (Supplementary Figs. 17 and 18) as previously reported

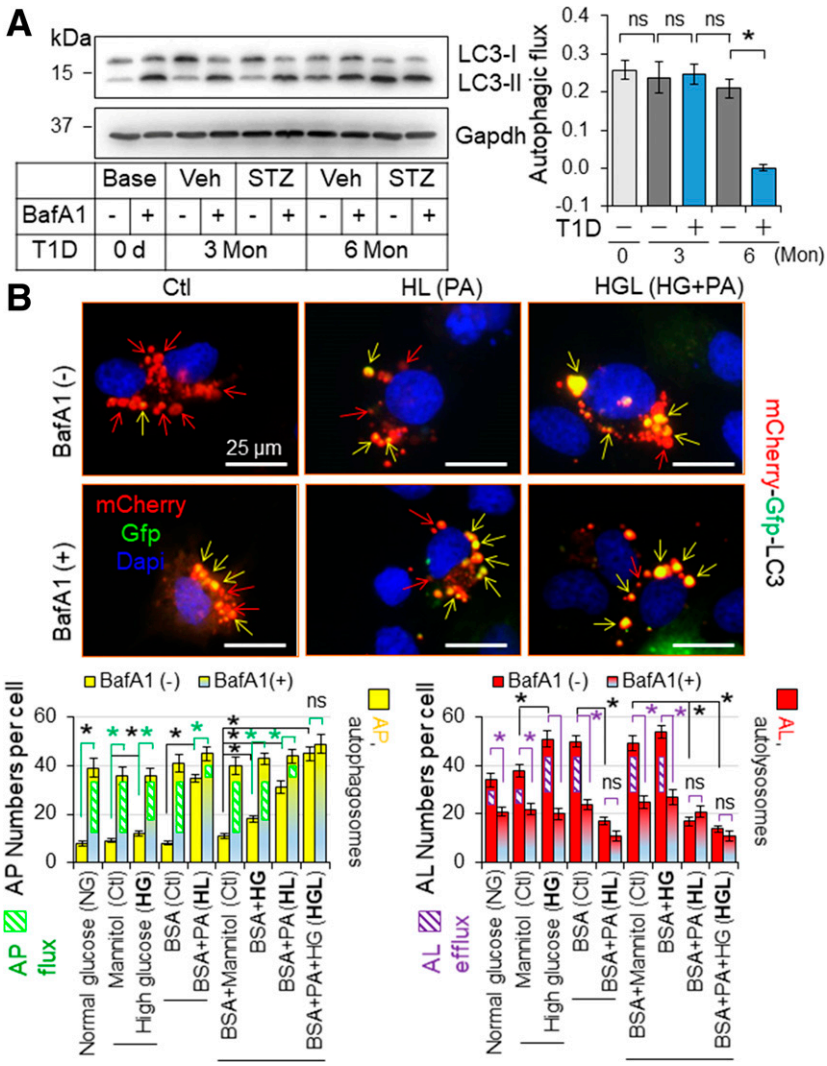

Figure 3—The impact of T1D on myocardial autophagy in mice. *A*: The impact of T1D on cardiac autophagic flux in mice. T1D in adult male mice on a FVB/N genetic background was induced by i.p. injection of STZ for 6 months (Mon), and myocardial autophagic flux was assessed at indicated time points as described in RESEARCH DESIGN AND METHODS. *A*: Myocardial autophagy flux. The left panel shows the representative immunoblots, and the right panel shows the quantified results ($n = 4$). LVs of these mice were used for the assessment. *B:* The impact of diabetes settings on autophagy in H9C2 cardiomyocyte-like cells. H9C2 cells transfected with mCherry-Gfp-Lc3 reporter plasmids were treated with or without BafA1 (10 nmol/L) for 24 h under the culture conditions as described in RESEARCH DESIGN AND METHODS. AL, autolysosomes; AP, autophagosomes; HG, high glucose; HL, high lipid PA loading; ns, nonsignificant. *$P < 0.05$ between indicated groups.

(24). These results reveal that lipotoxicity or glucolipotoxicity, but not glucotoxicity alone, induces autophagy inhibition, and glucolipotoxicity is the most potent inducing factor of autophagy inhibition in cardiomyocytes. Given that intramyocardial lipid deposition is correlated with hyperlipidemia and it is aggravated over time in T1D (23), it is conceivable that both intramyocardial lipid overload and hyperglycemia, but not hyperglycemia alone, cause cardiac autophagy inhibition in T1D over time, indicating chronic glucolipotoxicity–induced myocardial autophagy inhibition in T1D.

Next, we examined the impact of CR-Atg5KO on cardiomyopathy associated with STZ-induced T1D in adult mice. To minimize the potential impact of tamoxifen-induced Cre expression per se on cardiac remodeling, we used Cre mice as the control (Ctl) as previously reported (19). We found that CR-Atg5KO had negligible impact on STZ-induced diabetes per se, which was evidenced by the comparable BW decreases, fasting blood glucose levels, and glucose tolerance in Ctl and CR-Atg5KO mice (Supplementary Fig. 19). However, CR-Atg5KO caused early onset of cardiac dysfunction and promoted its progression over time (Fig. 4*A* and *C*). CR-Atg5KO also significantly exacerbated diabetes-induced cardiac pathologies including cardiac fibrosis, hypertrophy, cell death, and oxidative stress (Fig. 4*B* and *C* and Supplementary Fig. 20). In addition, knockdown of Atg5 enhanced H9C2 cell death in a normal- or high-glucose milieu but not in a lipid-overloading or lipid-overloading with high-glucose milieu (Fig. 4*D*), indicating

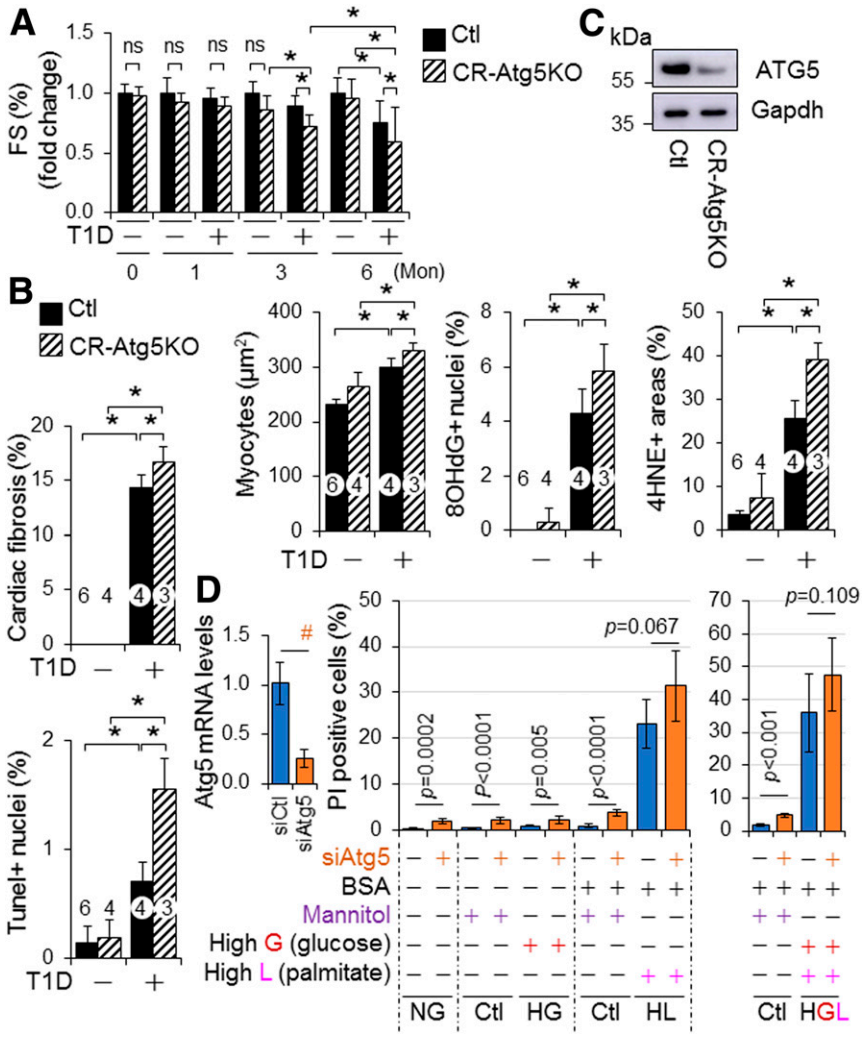

Figure 4—The role of cardiac autophagy in murine cardiomyopathy-associated STZ-induced diabetes. *A–C*: The impact of CR-Atg5KO on T1D-induced cardiomyopathy in mice. T1D in littermates of adult female MerCreMer^{+} Ctl and MerCreMer^{+}::Atg5$^{fl/fl}$ (CR-Atg5KO) mice on a C57BL/6J genetic background after tamoxifen induction was induced by i.p. injection of STZ for 6 months (Mon), and T1D-induced cardiomyopathy was assessed as described in RESEARCH DESIGN AND METHODS. *A*: Cardiac function. *B:* Cardiac remodeling, apoptosis, and oxidative stress. Cardiomyocyte sizes and cardiac fibrosis, apoptosis, and oxidative stress were assessed in LVs of 6-month diabetic MerCreMer^{+} Ctl and MerCreMer^{+}::Atg5$^{fl/fl}$ (CR-Atg5KO) mice after tamoxifen induction (n = 3–6). *C*: Tamoxifen-induced CR-Atg5 KO is confirmed by Western blot analysis using whole heart tissue lysates at each experimental end point. Animal numbers of each group in *A* are shown in Supplementary Fig. 19*A*. Animal numbers of each group in *B* are indicated in the parenthesis. *$P < 0.05$ between indicated groups. *D*: The impact of Atg5 knockdown on cell death in H9C2 cardiomyocyte-like cells under diabetes conditions. The set of experiments (n = 6) was carried out as described in RESEARCH DESIGN AND METHODS. #$P < 0.05$ between indicated groups. G, glucose; HG, high glucose to induce glucotoxicity; HGL, high glucose plus high lipid (PAs) loading to induce glucolipotoxicity; HL, high lipid (PAs) loading to induce lipotoxicity; L, lipid; NG, normal glucose.

that autophagy inhibition is a contributory mechanism of lipotoxicity and/or glucolipotoxicity in cardiomyocytes. To this end, these results demonstrate that T1D over time induces glucolipotoxicity-dependent cardiac cell death via myocardial autophagy inhibition, thereby contributing to the pathogenesis of diabetic cardiomyopathy.

Cardiac Autophagy Inhibition Is Critical for Driving Nrf2-Mediated Myocardial Damage in T1D

Given that *1*) Nrf2-mediated cardiac dysfunction was not observed at 3 months when myocardial autophagy is intact but appeared at 6 months when myocardial autophagy is inhibited in T1D (Figs. 1*C*, 3*A*, and 4*A*), *2*) cardiac autophagy inhibition exaggerated the progression of diabetic cardiomyopathy (Fig. 4*A–C*), and *3*) cardiac autophagy inhibition turned on Nrf2-mediated myocardial damage in the pressure-overloaded heart (19), we questioned whether cardiac autophagy inhibition is critical for driving Nrf2-mediated myocardial damage, thus promoting the progression of cardiomyopathy associated with T1D. Accordingly, we determined whether CR-Atg5KO activates Nrf2-mediated progression of cardiomyopathy associated

with STZ-induced T1D in adult mice. Since there is a clear progression of diabetic cardiomyopathy from 6 to 9 months after onset of diabetes induced by STZ in adult mice (Figs. 1 and 2), we chose 9 months after onset of diabetes as the end point for this set of experiments. As observed at 6 months after onset of diabetes (Fig. 4*A*–*C*), CR-Atg5KO enhanced diabetes-induced cardiac pathological remodeling and dysfunction (Fig. 5). As expected, these adverse phenotypes were significantly attenuated by additional Nrf2KO (Fig. 5). CR-Atg5KO did not affect the status of diabetes per se (data not shown). These results indicate an axis of autophagy inhibition–Nrf2 activation–cardiac damage and dysfunction in T1D.

Chronic T1D Induces Ferroptosis via Activating Nrf2 in Cardiomyocytes

A recent study documented that Nrf2 may play a mediator role in doxorubicin-induced ferroptosis, an iron-dependent form of regulated cell death that occurs through the lethal accumulation of lipid peroxides, in cardiomyocytes via upregulating heme oxygenase-1 (Ho-1) (25). Another report showed that myocardial ischemia/reperfusion injury enables cardiac myocytes to die of ferroptosis in a setting of T1D (26). Accordingly, we determined whether Nrf2 mediates myocardial ferroptosis in T1D induced by STZ in adult mice. Cardiac iron deposition was significantly increased at 9 months after onset of diabetes, and diabetes-induced iron deposition was enhanced by CR-Atg5KO; however, both increases were rescued by Nrf2KO (Fig. 6*A* and *B*). Considering that diabetes-induced changes of myocardial 4-hydroxy-2-nonenal (4HNE), a biomarker of lipid peroxidation for ferroptosis, exhibited a similar pattern in these mice (Figs. 2*E* and 5*C*), it is likely that Nrf2 promotes cardiomyocyte ferroptosis via enhancing iron deposition and lipid peroxidation in T1D. Indeed, knockdown of Nrf2 selectively suppressed glucolipotoxicity, while ferroptosis inhibitor ferrostatin-1 (Fer-1) and iron chelator deferoxamine inhibited glucolipotoxicity in H9C2 cells (Fig. 6*C*–*E*), suggesting that glucolipotoxicity occurring at the late stage of T1D drives Nrf2-mediated ferroptosis in cardiomyocytes. To this end, our results suggest an axis of chronic T1D–autophagy inhibition–Nrf2 activation–ferroptosis in cardiomyocytes.

To further confirm the Nrf2-mediated ferroptosis in cardiomyocytes, we characterized the role of Nrf2 in ferroptosis in cultured H9C2 cells, which was induced by erastin, an inhibitor of system x_c^-, that prevents cystine import and depletes glutathione, leading to inactivation of glutathione peroxidase 4 (GPX4), a crucial suppressor of lipid peroxidation–dependent ferroptosis (27). A dose-response study revealed that erastin at 5 μmol/L kills ~50% of the cells within 24 h, which is inhibited by ferroptosis inhibitor Fer-1 (Supplementary Fig. 21*A*), demonstrating erastin-induced ferroptosis in H9C2 cells. In agreement with previous studies, erastin upregulated the expression of ferroptosis biomarkers prostaglandin E synthase 2 (Ptgs2)/cyclooxygenase 2 (Cox2) and glutathione-specific γ-glutamylcyclotransferase 1 (Chac1) and downregulated expression of Gpx4 (27,28) while inducing accumulation of free iron as evidenced by upregulated gene expression of hepcidin antimicrobial peptide 1 (Hamp1), a free iron loading marker, transferrin receptor 1 (TfR1) for iron uptake protein, and ferritin H (FtH) and ferritin light chain 1 (Ftl1) for iron storage in cardiomyocytes (29,30) (Supplementary Fig. 21*B*). In addition, erastin upregulated gene expression of acyl-CoA synthetase long-chain family 4 (Acsl4) coding ACSL4, which is required for lipid peroxidation to induce ferroptotic cell death in a setting of GPX4 inhibition (31) while downregulating the expression of ferroptosis suppressor protein 1 (Fsp1), also known as apoptosis-inducing factor mitochondria 2 (Aifm2) coding FSP1, a glutathione-independent inhibitor of ferroptosis, that functions as an oxidoreductase to reduce coenzyme Q10 for halting the propagation of lipid peroxides (32,33) (Supplementary Fig. 21*B*). Moreover, it upregulated the expression of Nrf2 as well as its target genes including antioxidant NAD(P)H quinone dehydrogenase 1 (Nqo1), Cd36 and angiotensinogen (Agt) (10,13,34), and Kruppel-like factor (Klf)9 (35) (Supplementary Fig. 21*B*). These results demonstrate that erastin induces ferroptosis via inactivating GPX4 and downregulating FSP1 while upregulating ACSL4 (Supplementary Fig. 21*C*) associated with Nrf2 activation in H9C2 cells. Next, we determined the effect of Nrf2 knockdown on ferroptosis in H9C2 cells. Knockdown of Nrf2 slightly increased cell death (Fig. 7*A* and *B*) under the culture condition with normal glucose level, which maintains autophagy integrity (Fig. 3*B* and Supplementary Figs. 17 and 18), indicating a cytoprotective role of Nrf2 in cardiomyocytes with normal autophagy function. However, knockdown of Nrf2 strongly attenuated ferroptosis induced by erastin and oncogenic-RAS-selective lethal 3 (RSL3), a small molecule that acts as a GPX4 inhibitor to induce ferroptosis (36) (Fig. 7*A* and *B*), demonstrating Nrf2-mediated ferroptosis in a setting of GPX4 inactivation. Also, the inactivation of Nrf2 via knockdown of Nrf2 suppressed both basal and erastin-induced expression of Acsl4 but reversed erastin-induced repression of Fsp1 expression while upregulating its basal expression (Fig. 7*C*). These results uncover that Nrf2 drives Acsl4 expression while repressing Fsp1 in cardiomyocytes, which may be intensified in a setting of GPX4 inactivation leading to ferroptosis. Of interest, erastin inhibited autophagic flux (Fig. 7*D* and *E*), suggesting a contribution of autophagy inhibition in Nrf2-mediated ferroptosis in cardiomyocytes.

Taken together, our findings indicate that T1D-induced autophagy inhibition may activate Nrf2-mediated ferroptosis in cardiomyocytes, thereby contributing to the progression of diabetic cardiomyopathy.

Nrf2-Driven Defense Is Compromised While Nrf2-Operated Pathological Signaling Is Activated in Autophagy-Impaired Diabetic Hearts

To determine whether the observed phenotypes associated with Nrf2KO in T1D are caused by noncardiac effects of

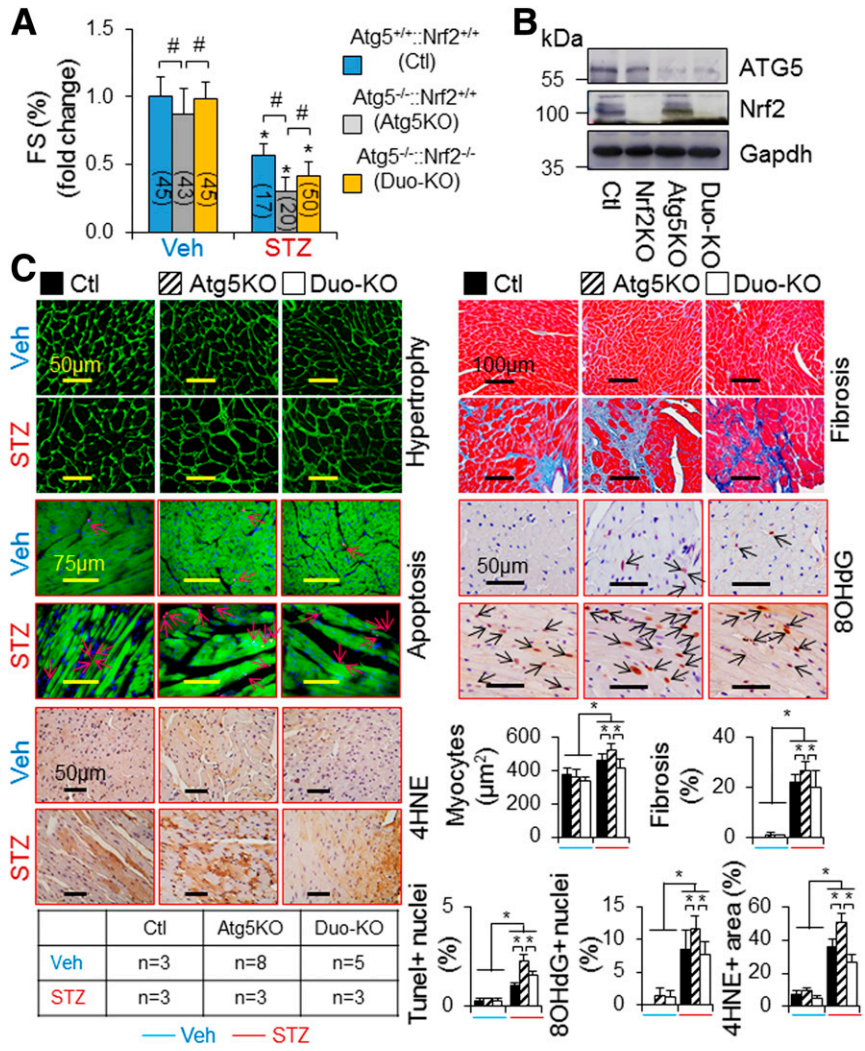

Figure 5—The impact of Nrf2KO on CR-Atg5KO–exaggerated cardiomyopathy associated with STZ-induced diabetes in mice. T1D in littermates of adult female MerCreMer^{+} Ctl and MerCreMer^{+}::Atg5$^{fl/fl}$ (CR-Atg5KO) mice on a C57BL/6J genetic background after tamoxifen induction was induced by i.p. injection of STZ for 9 months, and T1D-induced cardiomyopathy was assessed as described in RESEARCH DESIGN AND METHODS. *A*: Cardiac function. *$P < 0.05$ vs. vehicle (Veh) Ctl in the same groups; #$P < 0.05$ between indicated groups. *B*: Tamoxifen-induced CR-Atg5KO is confirmed by Western blot analysis with use of whole LV tissue lysates at the experimental end point. *C*: Cardiac remodeling, apoptosis, and oxidative stress. Cardiomyocyte sizes and cardiac fibrosis, apoptosis, and oxidative stress were assessed in LVs of MerCreMer^{+} Ctl, MerCreMer^{+}::Atg5$^{fl/fl}$ (Atg5KO), and MerCreMer^{+}::Atg5fl/fl::Nrf2KO (Duo-KO) mice after tamoxifen induction at 9 months after onset of diabetes. Animal numbers of each group are shown in the inserted table. *$P < 0.05$ between indicated groups.

Nrf2 or potential compensatory responses due to global Nrf2KO, we studied the impact of CR-Nrf2 overexpression on the cardiomyopathy associated with STZ-induced T1D using littermates of NG and TG mice on a FVB/N genetic background. STZ-induced hyperglycemia was comparable in wild-type FVB/N and C57BL/6J mice (Supplementary Figs. 1*C* and 22*B*). Diabetes-induced cardiac dysfunction of NG mice appeared at 5 months (Fig. 8*A* and Supplementary Fig. 22*D*), which is similar to wild-type mice on a C57BL/6J genetic background (Fig. 1*C*). Diabetes-induced cardiomyocyte hypertrophy and death in NG mice (Supplementary Fig. 22*E*–*G*) were comparable with those in wild-type C57BL/6J mice (Fig. 2). However, diabetes-induced cardiac fibrosis and oxidative DNA damage (8-hydroxy-2′-deoxyguanosine [8OHdG] staining), but not lipid peroxidation (4HNE staining) (Fig. 8*B*), were less in NG mice (Supplementary Fig. 22*F*–*H*) compared with wild-type C57BL/6J mice (Fig. 2). These results reveal that the genetic background has a marginal effect on hyperglycemia per se and diabetes-induced cardiac dysfunction but affects the pathogenesis of cardiac remodeling in T1D. Nevertheless, the common pathways toward cardiomyopathy in type 1 diabetes–independent genetic backgrounds may include lipid peroxidation and cell death in cardiomyocytes. Accordingly, we further observed that CR-Nrf2 overexpression had minimal impact on diabetes per se (Supplementary Fig. 22*A* and *B*) and the onset of cardiac dysfunction at 5 months but worsened cardiac dysfunction

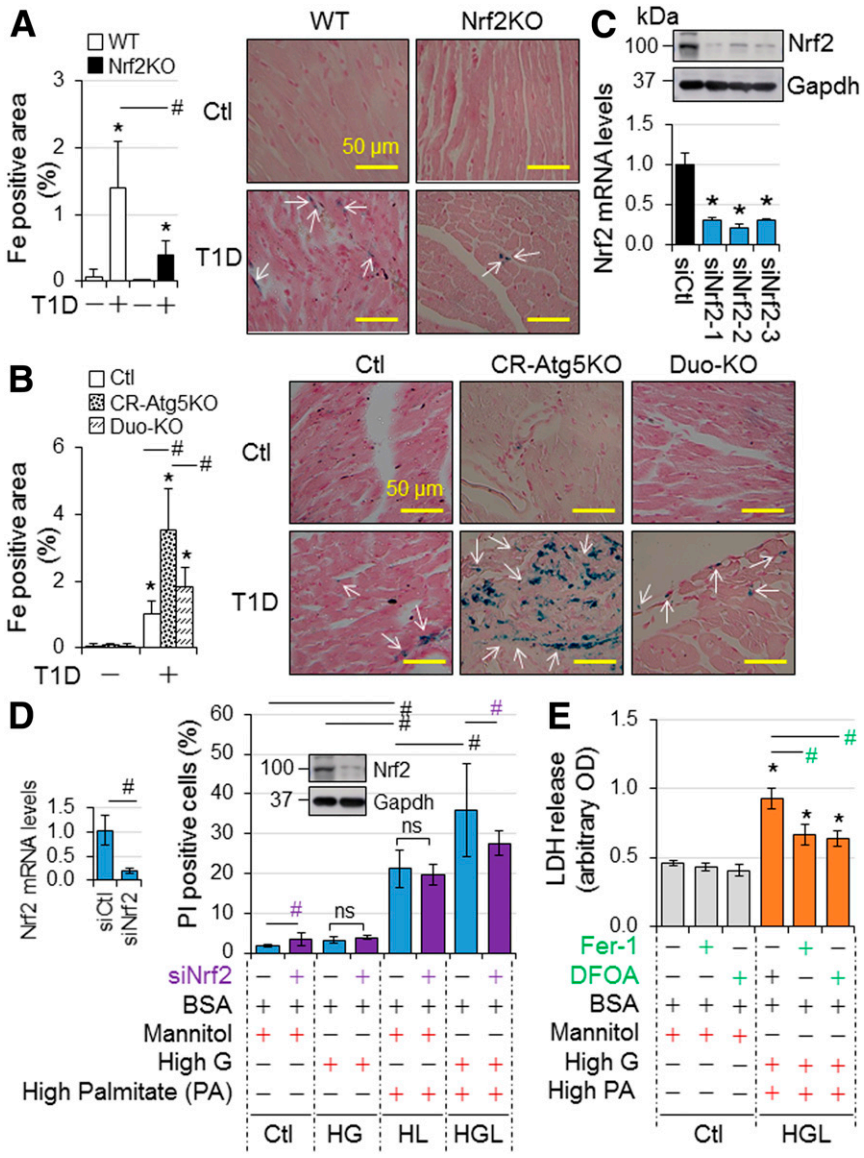

Figure 6—A potential axis of autophagy inhibition–Nrf2 activation–ferroptosis in cardiomyocytes induced by T1D. *A*: The impact of Nrf2KO on murine myocardial iron deposition in T1D. Iron deposition in LVs of adult male WT and Nrf2KO mice at 9 months after onset of T1D in Fig. 1 ($n = 4$) was quantified as described in RESEARCH DESIGN AND METHODS. *B*: The impact of Nrf2KO on CR-Atg5KO–exacerbated murine myocardial iron deposition in T1D. Iron deposition in LVs of adult female MerCreMer^{+} Ctl, CR-Atg5KO, and CR-Atg5KO and Nrf2KO (Duo-KO) mice at 9 months after onset of T1D in Fig. 5 ($n = 3$) was quantified as described in RESEARCH DESIGN AND METHODS. *C*: Efficiency of siNrf2 in knocking down Nrf2 in H9C2 cardiomyocyte-like cells. Upper panel shows the representative immunoblotting of Nrf2. Lower panel shows qPCR analysis of Nrf2 mRNA expression ($n = 4$). *$P < 0.05$ vs. siCtl (siRNA Ctl). Accordingly, siNrf2-2 was selected for the experiment of *D*. *D*: The effect of Nrf2 knockdown on H9C2 cell death in diabetes settings ($n = 6$). *E*: High-glucose and lipid milieu–induced ferroptosis in H9C2 cells ($n = 4$). DFOA, deferoxamine; HG, high glucose; HGL, high glucose plus high lipid (PAs) loading to induce glucolipotoxicity; HL, high PA loading. All experimental procedures are described in RESEARCH DESIGN AND METHODS. *$P < 0.05$ vs. Ctl in the same groups; #$P < 0.05$ between indicated groups.

at 7 months associated with increased death rate (Fig. 8*A* and Supplementary Fig. 22*C* and *D*). Diabetes-induced cardiac fibrosis, oxidative stress, and apoptosis, but not cardiomyocyte hypertrophy, were enhanced by CR-Nrf2 overexpression (Supplementary Fig. 22*E*–*H*). Notably, enhanced oxidative stress appears to be the most obvious impact of CR-Nrf2 overexpression on the diabetic heart. These results reveal that activation of cardiac Nrf2 may not be beneficial; instead, it could be detrimental to the diabetic heart via a mechanism to increase cardiac oxidative stress, thereby contributing to the progression of diabetic cardiomyopathy. To further dissect the relationship between cardiac autophagy inhibition and Nrf2 adverse activation in T1D-induced cardiomyopathy, we determined the effect of CR-Nrf2 overexpression on the dynamics of myocardial autophagy inhibition and downregulation of

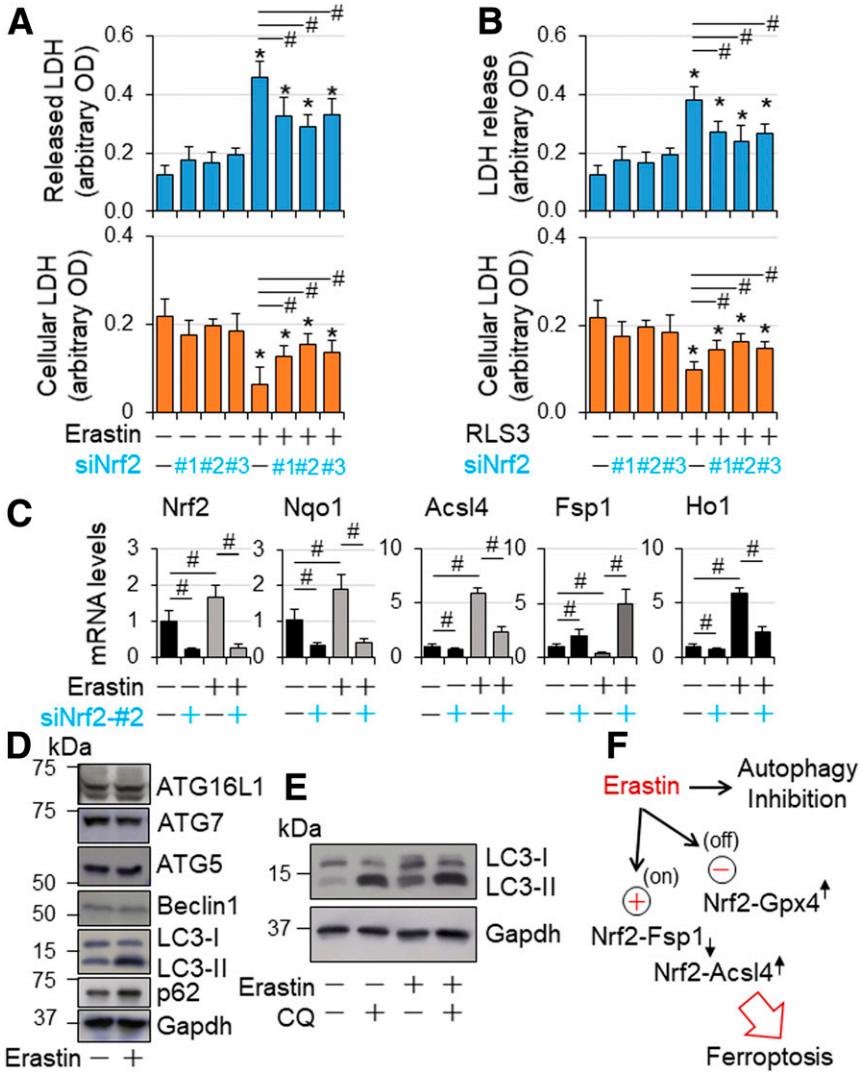

Figure 7—Nrf2-mediated ferroptosis in H9C2 cardiomyocyte-like cells. *A* and *B*: The effect of Nrf2 knockdown on ferroptosis in H9C2 cardiomyocyte-like cells. H9C2 cells transfected with siCtl and siNrf2 RNAs as described in Fig. 6*C* were treated with or without erastin (5 μmol/L) and RSL3 (5 μmol/L) as indicated in serum-free DMEM for 24 h and then subjected to cytotoxicity assay as described in RESEARCH DESIGN AND METHODS. $n = 4$. *$P < 0.05$ vs. vehicle-treated groups; #$P < 0.05$ between indicated groups. *C*: The effect of Nrf2 knockdown on mRNA expression of Nrf2, Nqo1, Fsp1, and Acsl4 in a setting of GPX4 inactivation in H9C2 cardiomyocyte-like cells. H9C2 cells transfected with siCtl and siNrf2 RNAs as described in Fig. 6*D* were treated with or without erastin (5 μmol/L) as indicated in serum-free DMEM for 24 h and then subjected to qPCR analysis of mRNA expression as described in RESEARCH DESIGN AND METHODS. $n = 4$. #$P < 0.05$ between indicated groups. *D*: The effect of erastin on protein expression of autophagic genes in H9C2 cardiomyocyte-like cells. Subconfluent H9C2 cells were treated with or without erastin (5 μmol/L) in serum-free DMEM for 24 h and then subjected to Western blot analysis as described in RESEARCH DESIGN AND METHODS. The results are representatives of four separated experiments. *E*: The effect of erastin on autophagic flux in H9C2 cardiomyocyte-like cells. Subconfluent H9C2 cells were treated with or without erastin (5 μmol/L) in serum-free DMEM for 24 h, and chloroquine (200 μmol/L) was added during the last 2 h of culture. Autophagic flux was assessed by Western blot analysis as described in RESEARCH DESIGN AND METHODS. The results are representatives of four separated experiments. *F*: A working hypothesis. In a setting of GPX4 inaction and autophagy inhibition, such as erastin treatment, Nrf2 drives the expression of ferroptosis executor Acsl4 while suppressing the expression of ferroptosis inhibitor Fsp1, thereby promoting ferroptosis in cardiomyocytes.

autophagy-related gene expression associated with STZ-induced T1D in mice. We found that CR-Nrf2 overexpression hardly affected the dynamics of autophagy inhibition and minimally regulated the downregulation of several autophagy genes including Atg5, Atg7, Atg12, and Atg16l1; Ras genes from rat brain 7 (Rab7) and Rab9; and lysosomal-associated membrane protein 1 (Lamp1) (Supplementary Fig. 23). Collectively, these results suggest that the detrimental activation of cardiac Nrf2 is most likely secondary to myocardial autophagy inhibition in T1D.

Next, we determined whether Nrf2-operated ferroptotic signaling in autophagy-impaired H9C2 cells could be recapitulated in the pathogenesis of cardiomyopathy associated with STZ-induced T1D in mice. We first characterized myocardial expression patterns of ferroptosis-related genes as well as Nrf2 and its target genes over

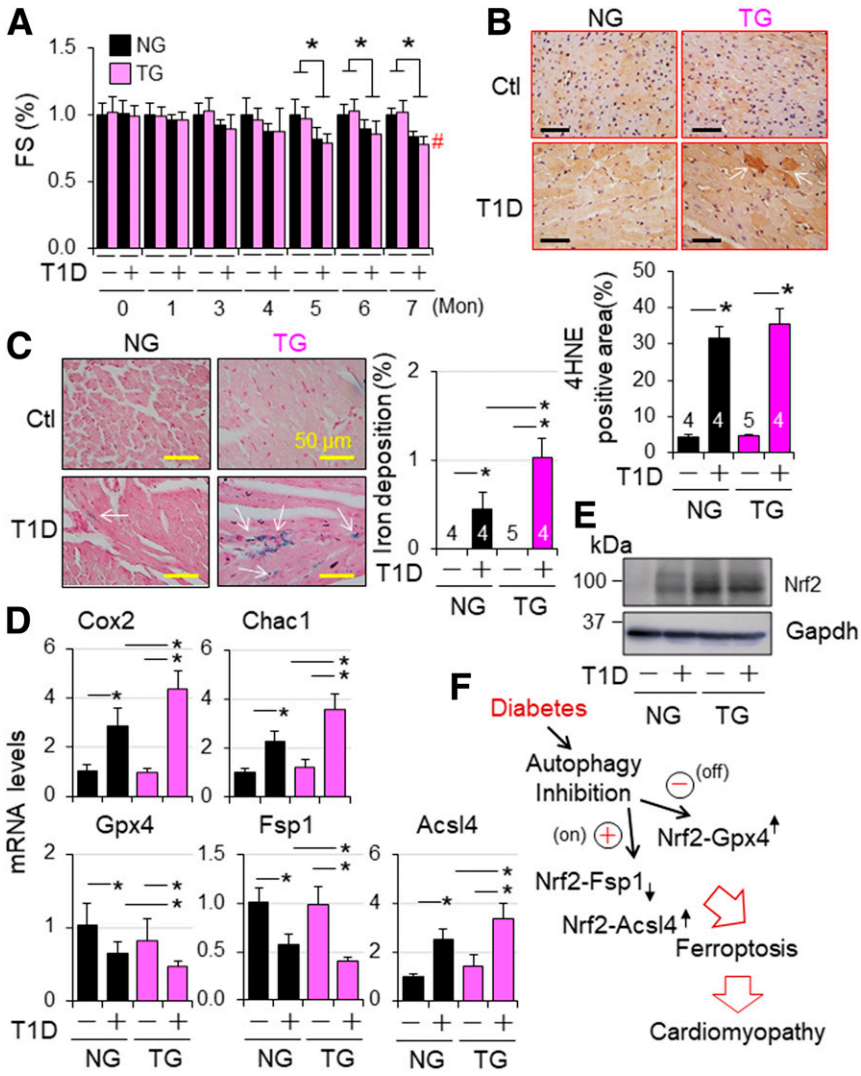

Figure 8—Nrf2-operated myocardial anti- and proferroptotic signaling in type 1 diabetic mice. T1D in adult female NG and TG mice was induced by i.p. injection of STZ as described in RESEARCH DESIGN AND METHODS. Animal numbers of each group are shown in Supplementary Fig. 22*C*. *A*: Cardiac function. Cardiac function was monitored monthly. FS (%) in fold changes. FS (%) of vehicle-treated NG and TG groups are set as onefold. *$P < 0.05$ between indicate groups; #$P < 0.05$ vs. STZ NG group at 7 months. *B*: Myocardial 4HNE staining at 7 months after onset of T1D. *C*: Myocardia iron staining at 7 months after onset of T1D. $n = 3$. *$P < 0.05$ between indicated groups. *D*: The effect of CR-Nrf2 overexpression on T1D-induced ferroptotic signaling. T1D in adult male NG and TG mice was induced by i.p. injection of STZ for 6 months, and myocardial expression of ferroptotic signaling genes was assessed by qPCR analysis ($n = 4$). *$P < 0.05$ between indicated groups. *E*: Western blot analysis of myocardial Nrf2 expression in NG and TG mice at 6 months after onset of diabetes. The results are representatives of four separated experiments. LVs of adult male NG and TG mice at 6 months after onset of diabetes were harvested for qPCR (*D*) and Western blot analyses (*E*). *F*: A working hypothesis. Diabetes over time impairs myocardial autophagy, which in turn inactivates Nrf2-operated antioxidant defense, such as GPX4 expression, while intensifying an Nrf2-driven pathological gene program, such as upregulation of ACSL4 to promote lipid peroxidation for ferroptosis, thereby promoting the progression of diabetic cardiomyopathy.

time in adult wild-type FVB/N mice with STZ-induced diabetes. At 3 months after onset of diabetes when myocardial autophagy was intact (Fig. 3*A*), the expression of ferroptosis markers, Cox2 and Chac1, was upregulated, while the expression of ferroptosis inhibitors, Gpx4 and Fsp1, was downregulated (Supplementary Fig. 24*A*), suggesting potential onset of cardiac ferroptosis. This notion is supported by the upregulated expression of Hamp1, indicating increased iron loading in the heart (30), which may promote ferroptosis (37). The increased iron loading is likely occurring within mitochondria as evidenced by the upregulation of mitochondria iron importer mitoferrin 2 (Mfrn2) and iron storage Fth1 associated with the downregulation of iron uptake (Tfr1) and the upregulation of iron transporter ferroportin-1 (Fpn1) (Supplementary Fig. 24*A* and *B*). In addition, the expression of Nrf2 and its target genes was upregulated, including antioxidant Nqo1 and Ho-1, Cd36 and Agt which are capable of damaging diabetic myocardium (10,13,34), and Klf9 which is responsible for cell death in response to excessive oxidative

stress (35), a common downstream event of CD36 and AGT signaling in diabetic cardiac remodeling (13,38) (Supplementary Fig. 24*C* and *D*). A repressor effect of Nrf2 on the expression of cardiac-protective Fgf21 (13) was also reserved in the diabetic heart (Supplementary Fig. 24*C* and *D*). These results suggest that Nrf2 signaling is fully activated in the diabetic heart, and the preserved cardiac function may reflect a net effect balanced between Nrf2-driven cellular defense and an Nrf2-operated damaging program in the diabetic heart with intact autophagy. At 6 months after onset of diabetes, when myocardial autophagy is inhibited (Fig. 3*A*), we noticed that a major difference in the gene expression profile is the upregulation of ferroptosis executor Acsl4, and it (Supplementary Fig. 24) almost mirrored that of H9C2 cells undergoing ferroptotic cell death induced by erastin (Supplementary Fig. 21), indicating the intensified ferroptosis in autophagy impaired diabetic hearts. Therefore, we then examined lipid peroxidation and iron deposition, as well as the expression of ferroptosis biomarkers, Cox2 and Chac1; ferroptosis inhibitors, Gpx4 and Fsp1; and the ferroptosis executor Acsl4 in littermate hearts of NG and TG mice at 7 months after onset of T1D induced by STZ. In the diabetic and dysfunctional hearts with autophagy inhibition (Figs. 3*A* and 8*A*), CR-Nrf2 overexpression enhanced lipid peroxidation (increased accumulation of focal 4HNE), iron deposition, and the expression of Cox2, Chac1, and Acsl4 while suppressing Gpx4 and Fsp1 (Fig. 8*B–D*). These findings support the notion that autophagy inhibition activates Nrf2 to promote ferroptosis in cardiomyocytes in chronic diabetic hearts (Fig. 8*E*).

DISCUSSION

In the current study, we have uncovered a temporal regulation of Nrf2 signaling in enhancing ferroptosis, thereby exacerbating diabetic cardiomyopathy. Normally, Nrf2 maintains metabolic and redox homeostasis by controlling the expression of selected sets of genes involved in iron and lipid metabolism, and redox balance in the heart. However, the Nrf2-governed metabolic and redox balance is interrupted when myocardial autophagy becomes insufficient, presumably at a stage of autolysosome efflux during a chronic stage of T1D. The net outcome of interrupted Nrf2-driven signaling is most likely to promote ferroptosis in cardiomyocytes, thereby exaggerating the progression of cardiomyopathy in T1D. These findings not only help explain the controversial observations regarding the role of Nrf2 and autophagy in diabetic hearts but also provide novel insights into the pathogenesis of diabetic cardiomyopathy.

STZ at high doses has off-target effects causing extrapancreatic genotoxic effects; therefore, AMDCC has recommended the low-dose protocol of STZ (five consecutive i.p. injections of 50 mg/kg/day STZ) for establishing a mouse model of T1D (21). Notably, the controversial phenotypes of global Nrf2KO mice in STZ-induced T1D mice are actually associated with the doses of STZ used in these studies (11,12,39,40). Global Nrf2KO exaggerated a high dose of STZ (150 or 200 mg/kg by a single i.p. injection)–induced hyperglycemia (11,39) while suppressing a low dose of STZ (50 mg/kg/day, i.p. injection for five consecutive days)–induced hyperglycemia (40) in mice with the same genetic background. Importantly, global Nrf2KO worsened diabetic cardiomyopathy in mice that received high doses of STZ (11,12). However, cardiac protection may be achieved by downregulation of the Nrf2-Cd36 axis in diabetic Fgf21KO mice injected with a low dose of STZ (60 mg/kg/day for six consecutive days) (13). Accordingly, the adverse phenotypes of Nrf2KO mice associated with STZ-induced T1D most likely resulted from the off-target effects of STZ at high doses. In this regard, the current study using the low-dose protocol of STZ confirmed a mediator role of Nrf2 in promoting hyperglycemia. In addition, our results demonstrate that Nrf2 is not an inhibitor but, rather, is a mediator of the cardiomyopathy associated with T1D. Moreover, any doses of STZ >60 mg/kg/day for five consecutive days might cause off-target effects that affect cardiac phenotypes associated T1D.

Autophagy has been shown to be either cardiac protective or detrimental in T1D. To date, the detrimental role of autophagy in T1D-induced cardiomyopathy has been proposed mainly based on the observations of improved cardiac pathological remodeling and dysfunction associated with STZ-induced T1D in mice with Beclin-1 heterozygote deficiency or Atg16l1 hypomorphic allele (41). However, the genetic downregulation of Beclin-1 or Atg16l1 expression had almost no impact on myocardial autophagy flux under either a normal or type 1 diabetes condition (41). Notably, Beclin-1 can mediate cell death and may either promote or inhibit autophagy via the formation of signaling complex with ATG14L or Rubicon (14), respectively. However, the potential contribution of Beclin-1–mediated cell death or autophagy inhibition to T1D-induced cardiomyopathy has not been clarified. In addition, Atg16l1 hypomorphic allele can confer cellular protection by increasing the number of lysosomes (42,43). Nevertheless, whether the Atg16l1 deficiency improves lysosome function in the cardiomyopathy associated with T1D has remained unstudied. Moreover, the dynamics and nature of myocardial autophagy inhibition in T1D remain unclear (16,17). If myocardial autophagy inhibition in T1D occurs at the stage of autolysosome efflux, it is possible that the Beclin-1– or ATG16L1–mediated increases in autophagosome synthesis (41) may eventually become cytotoxic in cardiomyocytes as we observed in pressure-overloaded hearts of CR-Cyld (cylindromatosis) Tg mice (22). Therefore, it is still far from a comprehensive understanding of the role of autophagy in T1D-induced cardiomyopathy. In this regard, the current study reveals that chronic glucolipotoxicity (23,24), but not glucotoxicity alone, causes cardiac autophagy inhibition, most likely at the stage of autolysosome efflux in T1D, and demonstrates that cardiac autophagy inhibition via CR-Atg5KO not only leads to an early onset of T1D-induced cardiomyopathy but also accelerates the disease

progression. These results underscore a maladaptive nature of cardiac autophagy inhibition in the cardiomyopathy associated with T1D, which is caused by a joined force of hyperglycemia and hyperlipidemia rather than hyperglycemia alone. Although not conclusive at this moment, these results also support our assumption that Beclin-1 or ATG16L1 merely increases autophagosome synthesis without improving autolysosomal degradation to drive toxic accumulation of autophagosomes in type 1 diabetic hearts with impaired autolysosome efflux, thereby providing an alternative interpretation for Beclin-1– or ATG16L1-mediated diabetic cardiomyopathy (41). Because Nrf2KO could rescue CR-Atg5KO–dependent adverse phenotypes, it is conceivable that chronic T1D suppresses cardiac autophagy, thereby activating a unique Nrf2-operated signaling to promote progression of diabetic cardiomyopathy.

One striking finding of the current study is a critical role of Nrf2 in mediating glucolipotoxicity-dependent ferroptosis in H9C2 cardiomyocytes. At the molecular level, it is most likely that glucolipotoxicity causes ferroptosis in cardiomyocytes via activating Nrf2-driven transcription of Acsl4 and repression of Fsp1 expression while suppressing Nrf2-operating transcription of Gpx4 and impairing an Nrf2-coordinated gene network of iron metabolism, thereby facilitating the progression of diabetic cardiomyopathy. In addition, our observations that chronic type 1 diabetic hearts with autophagy inhibition phenocopied Nrf2-mediated ferroptosis in autophagy-impaired H9C2 cells indicate that Nrf2-mediated ferroptosis in cardiomyocytes is likely a downstream event of myocardial autophagy inhibition leading to the progression of cardiomyopathy in T1D over time. These results also highlight a unique role of Nrf2 in fine-tuning the fate of cardiomyocytes via balancing the expression of genes with opposite functions in regulating cell death. The observed Nrf2-mediated dichotomous actions are likely due to the potential dysregulation of Nrf2-driven gene expression in diverse pathophysiological settings. Our findings help explain the Nrf2-mediated cytotoxicity in cardiomyocytes induced by paraquat (44), which appears to be a potential inducer of the ferroptosis (45).

There are several issues requiring future studies. Firstly, whether the Nrf2-mediated dichotomy is restricted to T1D needs to be clarified. This question may be answered by determining the impact of CR-Atg5KO and Nrf2KO on cardiac pathological remodeling and dysfunction associated with obesity, which are induced by a 9-month high-fat diet in mice, a type 2 diabetes setting (46). Secondly, the discrepancies between the current study, which uncovered Nrf2-mediated myocardial damage, and the other studies, which showed Nrf2-mediated cardiac protection using a substantial number of natural compounds such as sulforaphane and resveratrol in animal models of diabetes (47), remain to be reconciled. However, it is worthy to note that not only the Nrf2 signaling but also the activation of myocardial autophagy are critical for the therapeutic effects of sulforaphane and resveratrol on diabetic cardiomyopathy (48,49). A plausible explanation is that the Nrf2-operated detrimental signaling is selectively terminated by the autophagy activation induced by these natural products including sulforaphane and resveratrol in diabetic hearts. Thirdly, whether autophagy-independent functions of ATG5 (50) play a role in the pathogenesis of diabetic cardiomyopathy or the activation of Nrf2-mediated pathological gene program in T1D is intriguing. Finally, the molecular mechanisms by which T1D induces cardiac autophagy inhibition and how the cardiac autophagy inhibition downregulates Nrf2-mediated defense while switching on an Nrf2-operated pathological gene program toward ferroptosis in the heart have not been fully delineated in the current study. As the enthusiasm for activating Nrf2 as a novel approach to treat human diseases, at least noncardiac diseases, remains high, several clinical trials of various phases on Nrf2 activators for treating several other forms of disease are still actively ongoing (4). Further investigation of these subjects will not only lead to a better understanding of the unique coupling between autophagy function and Nrf2 signaling in the pathogenesis of diabetic cardiomyopathy but also provide new insights into rational design and development of therapeutic approaches targeting Nrf2 to treat the diseases with conditions, such as hypertensive, ischemic, and diabetic cardiomyopathies, that all likely have myocardial autophagy inhibition (14,16,17).

Funding. This study was supported by the American Diabetes Association (1-16-IBS-059) and the National Institutes of Health (National Center for Complementary and Alternative Medicine [P01 AT003961], National Heart, Lung, and Blood Institute [R01 HL131667], and National Institute of Arthritis and Musculoskeletal and Skin Diseases [R01 AR073172]).

Duality of Interest. No potential conflicts of interest relevant to this article were reported.

Author Contributions. H.Z., W.W., L.Q., W.T., M.N., P.N., X.W., and T.C. approved the final version of the manuscript. H.Z. drafted the original manuscript. H.Z., W.W., and L.Q. performed experiments. H.Z. analyzed the data and created the figures. W.T., M.N., P.N., X.W., and T.C. covered the funding. T.C. designed the study and reviewed and edited the writing. T.C. is the guarantor of this work and, as such, had full access to all the data in the study and takes responsibility for the integrity of the data and the accuracy of the data analysis.

Prior Presentation. Parts of this study were presented in abstract form at the 78th Scientific Sessions of the American Diabetes Association, Orlando, FL, 22–26 June 2018.

References

1. Bugger H, Abel ED. Molecular mechanisms of diabetic cardiomyopathy. Diabetologia 2014;57:660–671

2. Huynh K, Bernardo BC, McMullen JR, Ritchie RH. Diabetic cardiomyopathy: mechanisms and new treatment strategies targeting antioxidant signaling pathways. Pharmacol Ther 2014;142:375–415

3. Khullar M, Al-Shudiefat AA, Ludke A, Binepal G, Singal PK. Oxidative stress: a key contributor to diabetic cardiomyopathy. Can J Physiol Pharmacol 2010;88:233–240

4. Zang H, Mathew RO, Cui T. The dark side of Nrf2 in the heart. Front Physiol 2020;11:722

5. Li J, Ichikawa T, Janicki JS, Cui T. Targeting the Nrf2 pathway against cardiovascular disease. Expert Opin Ther Targets 2009;13:785–794

6. Uruno A, Furusawa Y, Yagishita Y, et al. The Keap1-Nrf2 system prevents onset of diabetes mellitus. Mol Cell Biol 2013;33:2996–3010

7. Xu J, Kulkarni SR, Donepudi AC, More VR, Slitt AL. Enhanced Nrf2 activity worsens insulin resistance, impairs lipid accumulation in adipose tissue, and increases hepatic steatosis in leptin-deficient mice. Diabetes 2012;61:3208–3218
8. Xue P, Hou Y, Chen Y, et al. Adipose deficiency of Nrf2 in ob/ob mice results in severe metabolic syndrome. Diabetes 2013;62:845–854
9. Jiang T, Huang Z, Lin Y, Zhang Z, Fang D, Zhang DD. The protective role of Nrf2 in streptozotocin-induced diabetic nephropathy. Diabetes 2010;59:850–860
10. Zhao S, Ghosh A, Lo CS, et al. Nrf2 deficiency upregulates intrarenal angiotensin-converting enzyme-2 and angiotensin 1-7 receptor expression and attenuates hypertension and nephropathy in diabetic mice. Endocrinology 2018;159:836–852
11. He X, Ma Q. Disruption of Nrf2 synergizes with high glucose to cause heightened myocardial oxidative stress and severe cardiomyopathy in diabetic mice. J Diabetes Metab 2012;(Suppl. 7)7:002
12. Gu J, Cheng Y, Wu H, et al. Metallothionein is downstream of Nrf2 and partially mediates sulforaphane prevention of diabetic cardiomyopathy. Diabetes 2017;66:529–542
13. Yan X, Chen J, Zhang C, et al. FGF21 deletion exacerbates diabetic cardiomyopathy by aggravating cardiac lipid accumulation. J Cell Mol Med 2015;19:1557–1568
14. Wang X, Cui T. Autophagy modulation: a potential therapeutic approach in cardiac hypertrophy. Am J Physiol Heart Circ Physiol 2017;313:H304–H319
15. Linton PJ, Gurney M, Sengstock D, Mentzer RM Jr., Gottlieb RA. This old heart: cardiac aging and autophagy. J Mol Cell Cardiol 2015;83:44–54
16. Kobayashi S, Liang Q. Autophagy and mitophagy in diabetic cardiomyopathy. Biochim Biophys Acta 2015;1852:252–261
17. Ouyang C, You J, Xie Z. The interplay between autophagy and apoptosis in the diabetic heart. J Mol Cell Cardiol 2014;71:71–80
18. Zhang Y, Whaley-Connell AT, Sowers JR, Ren J. Autophagy as an emerging target in cardiorenal metabolic disease: from pathophysiology to management. Pharmacol Ther 2018;191:1–22
19. Qin Q, Qu C, Niu T, et al. Nrf2-mediated cardiac maladaptive remodeling and dysfunction in a setting of autophagy insufficiency. Hypertension 2016;67:107–117
20. Wang W, Li S, Wang H, et al. Nrf2 enhances myocardial clearance of toxic ubiquitinated proteins. J Mol Cell Cardiol 2014;72:305–315
21. Bugger H, Abel ED. Rodent models of diabetic cardiomyopathy. Dis Model Mech 2009;2:454–466
22. Qi L, Zang H, Wu W, et al. CYLD exaggerates pressure overload-induced cardiomyopathy via suppressing autolysosome efflux in cardiomyocytes. J Mol Cell Cardiol 2020;145:59–73
23. Ritchie RH, Zerenturk EJ, Prakoso D, Calkin AC. Lipid metabolism and its implications for type 1 diabetes-associated cardiomyopathy. J Mol Endocrinol 2017;58:R225–R240
24. Trivedi PC, Bartlett JJ, Perez LJ, et al. Glucolipotoxicity diminishes cardiomyocyte TFEB and inhibits lysosomal autophagy during obesity and diabetes. Biochim Biophys Acta 2016;1861:1893–1910
25. Fang X, Wang H, Han D, et al. Ferroptosis as a target for protection against cardiomyopathy. Proc Natl Acad Sci U S A 2019;116:2672–2680
26. Li W, Li W, Leng Y, Xiong Y, Xia Z. Ferroptosis is involved in diabetes myocardial ischemia/reperfusion injury through endoplasmic reticulum stress. DNA Cell Biol 2020;39:210–225
27. Stockwell BR, Friedmann Angeli JP, Bayir H, et al. Ferroptosis: a regulated cell death nexus linking metabolism, redox biology, and disease. Cell 2017;171:273–285
28. Hirschhorn T, Stockwell BR. The development of the concept of ferroptosis. Free Radic Biol Med 2019;133:130–143
29. Ganz T. Systemic iron homeostasis. Physiol Rev 2013;93:1721–1741
30. Lakhal-Littleton S, Wolna M, Chung YJ, et al. An essential cell-autonomous role for hepcidin in cardiac iron homeostasis. eLife 2016;5:e19804
31. Doll S, Proneth B, Tyurina YY, et al. ACSL4 dictates ferroptosis sensitivity by shaping cellular lipid composition. Nat Chem Biol 2017;13:91–98
32. Doll S, Freitas FP, Shah R, et al. FSP1 is a glutathione-independent ferroptosis suppressor. Nature 2019;575:693–698
33. Bersuker K, Hendricks JM, Li Z, et al. The CoQ oxidoreductase FSP1 acts parallel to GPX4 to inhibit ferroptosis. Nature 2019;575:688–692
34. Abdo S, Shi Y, Otoukesh A, et al. Catalase overexpression prevents nuclear factor erythroid 2-related factor 2 stimulation of renal angiotensinogen gene expression, hypertension, and kidney injury in diabetic mice. Diabetes 2014;63:3483–3496
35. Zucker SN, Fink EE, Bagati A, et al. Nrf2 amplifies oxidative stress via induction of Klf9. Mol Cell 2014;53:916–928
36. Yang WS, SriRamaratnam R, Welsch ME, et al. Regulation of ferroptotic cancer cell death by GPX4. Cell 2014;156:317–331
37. Anandhan A, Dodson M, Schmidlin CJ, Liu P, Zhang DD. Breakdown of an ironclad defense system: the critical role of NRF2 in mediating ferroptosis. Cell Chem Biol 2020;27:436–447
38. Kajstura J, Fiordaliso F, Andreoli AM, et al. IGF-1 overexpression inhibits the development of diabetic cardiomyopathy and angiotensin II-mediated oxidative stress. Diabetes 2001;50:1414–1424
39. Aleksunes LM, Reisman SA, Yeager RL, Goedken MJ, Klaassen CD. Nuclear factor erythroid 2-related factor 2 deletion impairs glucose tolerance and exacerbates hyperglycemia in type 1 diabetic mice. J Pharmacol Exp Ther 2010;333:140–151
40. Zheng H, Whitman SA, Wu W, et al. Therapeutic potential of Nrf2 activators in streptozotocin-induced diabetic nephropathy. Diabetes 2011;60:3055–3066
41. Xu X, Kobayashi S, Chen K, et al. Diminished autophagy limits cardiac injury in mouse models of type 1 diabetes. J Biol Chem 2013;288:18077–18092
42. Li J, Chen Z, Stang MT, Gao W. Transiently expressed ATG16L1 inhibits autophagosome biogenesis and aberrantly targets RAB11-positive recycling endosomes. Autophagy 2017;13:345–358
43. Wang C, Mendonsa GR, Symington JW, et al. Atg16L1 deficiency confers protection from uropathogenic Escherichia coli infection in vivo. Proc Natl Acad Sci U S A 2012;109:11008–11013
44. Wang S, Zhu X, Xiong L, Ren J. Ablation of Akt2 prevents paraquat-induced myocardial mitochondrial injury and contractile dysfunction: role of Nrf2. Toxicol Lett 2017;269:1–14
45. Rashidipour N, Karami-Mohajeri S, Mandegary A, et al. Where ferroptosis inhibitors and paraquat detoxification mechanisms intersect, exploring possible treatment strategies. Toxicology 2020;433–434:152407
46. Noyan-Ashraf MH, Shikatani EA, Schuiki I, et al. A glucagon-like peptide-1 analog reverses the molecular pathology and cardiac dysfunction of a mouse model of obesity. Circulation 2013;127:74–85
47. Parim B, Sathibabu Uddandrao VV, Saravanan G. Diabetic cardiomyopathy: molecular mechanisms, detrimental effects of conventional treatment, and beneficial effects of natural therapy. Heart Fail Rev 2019;24:279–299
48. Zhang Z, Wang S, Zhou S, et al. Sulforaphane prevents the development of cardiomyopathy in type 2 diabetic mice probably by reversing oxidative stress-induced inhibition of LKB1/AMPK pathway. J Mol Cell Cardiol 2014;77:42–52
49. Wang B, Yang Q, Sun YY, et al. Resveratrol-enhanced autophagic flux ameliorates myocardial oxidative stress injury in diabetic mice. J Cell Mol Med 2014;18:1599–1611
50. Galluzzi L, Green DR. Autophagy-independent functions of the autophagy machinery. Cell 2019;177:1682–1699